

# Autonomous Optical Sensing for Space-Based Space Surveillance

Khaja Faisal Hussain<sup>1</sup>, Kathiravan Thangavel<sup>2</sup>, Alessandro Gardi<sup>1,2</sup>, Roberto Sabatini<sup>1,2</sup>

<sup>1</sup>Department of Aerospace Engineering, Khalifa University of Science and Technology, Abu Dhabi, UAE

<sup>2</sup>School of Engineering, Aerospace Engineering and Aviation, RMIT University, Melbourne, VIC 3001, Australia

**Abstract**—Space debris population has increased dramatically in the past decades posing a threat to the future of space operations. Traditionally, Resident Space Objects (RSO) are tracked and catalogued using ground-based observations. However, Space Based Space Surveillance (SBSS) is a promising technology to complement the ground-based observations as it offers greater performance in terms of detectability, accuracy and weather independency. A Distributed Satellite System (DSS) architecture is proposed for a SBSS mission equipped with dual-use star trackers and inter-satellite communication links to interact and cooperate with each other to accomplish optimized RSO tracking tasks while assumed to simultaneously perform earth observation tasks. This paper focuses on stereovision-based tracking algorithms with higher detectability and tracking accuracy in SBSS tasks in order to identify an optimal tracking solution for Space Domain Awareness (SDA), which could support future Space Traffic Management (STM) operations. Navigation and tracking uncertainties are analyzed in representative conditions to support the optimal selection and processing of individual observations and to determine the actual confidence region around the detected objects. Additionally, Particle Swarm Optimization (PSO) is implemented on-board the satellites to grant the DSS autonomous trajectory planning and Collision Avoidance (CA) manoeuvring capabilities.

## TABLE OF CONTENTS

1. INTRODUCTION.....	1
2. AIM OF THE ARTICLE .....	3
3. SBSS MISSION ARCHITECTURE .....	3
4. SBSS TRACKING ALGORITHM .....	4
5. RESULTS AND DISCUSSIONS.....	6
6. CONCLUSION AND FUTURE WORK .....	8
REFERENCES.....	8
BIOGRAPHY .....	9

## 1. INTRODUCTION

The population of space debris has increased exceedingly in the past decade. Despite growing awareness of the orbital debris problem, recent developments such as growth in the availability of small launch vehicles and mega-constellation are majorly contributing to densifying orbital domain. Further exacerbating the space situation are a chain of undesirable events such as Anti-Satellite (ASAT) weapons tests, on orbit collisions, and satellite breakups[1]. Moreover, several commercial entities are planning to launch larger constellations (500–4,000 spacecraft each) in the coming days. Currently, the space domain usage is unsustainable. As

a result, the number of space objects will increase multifold due to a phenomenon called the Kessler Syndrome, resulting in the cessation of space activities in the near future. A recent ESA publication [2] emphasizes the alarming situation in the current space domain. Figure.1 illustrate the current space situation in terms of the number of launches and space debris population.

To prevent further collisions in Earth orbit, spacecraft operators need to possess a better awareness of the potential threats arising from the existing RSO (Resident Space Objects). This includes tracking, catalogue maintenance of RSO and continuously calculating the chances of other accidental collisions to avoid creating additional debris. Unfortunately, neither of these tasks is trivial and requires considerable tracking resources (Optical telescopes and radar), computing power, and sophisticated software to calculate numerous satellite–satellite or satellite–debris conjunctions on a daily basis. In space, these tasks are referred to as Space Domain Awareness (SDA). Currently, conventional satellite systems do not effectively contribute towards SDA because of their exclusive dependence on ground-based systems. Generally, these tasks are undertaken by the US Department of Defense (DoD)[3] through the Space Surveillance Network (SSN), a network of ground-based observation stations. Also contributing to SDA are a variety of ground-based space surveillance systems[4]. Even though these ground-based radars, lasers, and telescopes play an important role in providing SDA, it is still unclear whether they can effectively achieve this goal adapting to the rapidly evolving space domain for the following reasons.

- Most of the ground-based systems are able to perform regional surveillance and then randomly look at other areas.
- They lack persistence in surveillance. In order to achieve true surveillance, it is necessary to monitor objects or regions for extended periods of time.
- Due to space perturbations, there is an on-orbit change in the RSOs. This will decrease the revisit frequency of the RSO within the field of view of the sensors on the ground.
- Weather conditions are still a significant concern for ground-based systems. In typical ground-based observation sites, weather restricts visibility more than half the time, with some sites having a visibility of no more than 25%.
- Almost without exception, objects are extremely difficult to monitor as they pass between the Earth and the Sun. Daylight observations, in general, pose a significant challenge for ground-based optical sensors.

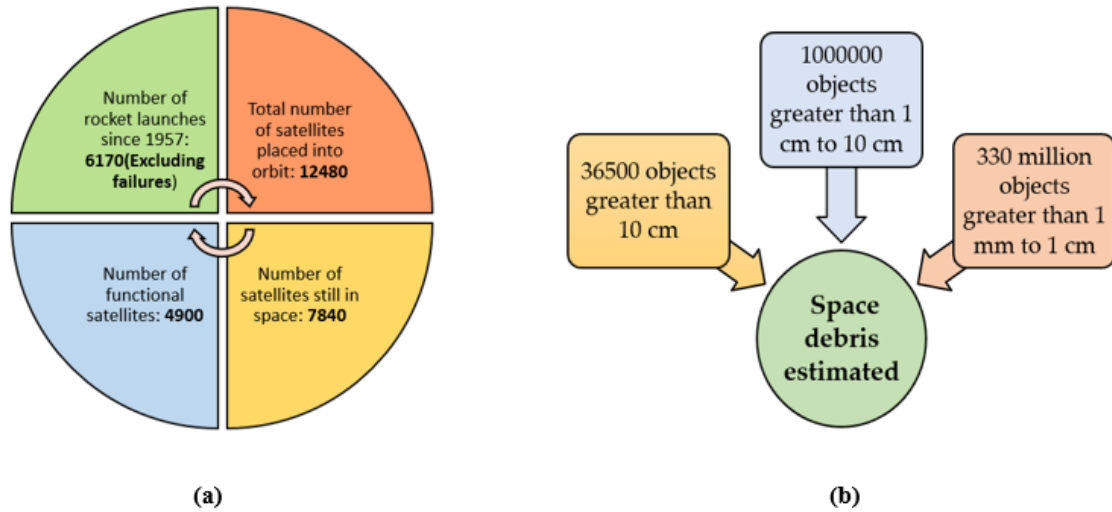


Figure 1: (a) Space environment statistics by ESA; (b) Space debris population estimation by ESA.

As a result of the gaps associated with ground-based measurements, it is possible to exploit spaceborne measurements to track RSOs [5] and this approach is termed as Space Based Space Surveillance (SBSS). SBSS is a successful solution because space-borne sensors provide better accuracy, a wider field of view, and weather independence. Further, space-based observation technologies are not affected by atmospheric scattering, turbulence, and aberrations [6]. SBSS has already been attempted in the past, the reader is directed to [7] which summarizes various SBSS missions attempted so far.

Space Traffic Management (STM) applications will continue to be increasingly dependent on accurate knowledge of the RSO's position and velocity. These estimations can be provided using two approaches. *Cooperative surveillance* relies on state estimates from on-board Time and Space Position Information (TSPI), navigation systems (e.g., GNSS, INS) and on the collaborative exchange of information among all other vehicles in the course of a potential collision. Whereas *Non-cooperative surveillance* is typically carried out by ground or space-based radar or electro-optical sensors that do not require communication with the observed object. These systems are prone to errors caused by physical phenomena or by the mathematical extrapolation itself. In other words, a non-cooperative scenario is described as an encounter between a host platform and an RSO or possibly a non-cooperative spacecraft, with only the host spacecraft capable of preventing a potential collision. A cooperative scenario, on the other hand, is described as all potentially colliding RSO being capable of communicating position data and, if necessary, averting collisions by conducting maneuvers[8].

Recent technological advances have led to the concept of multiple spacecraft operating in optimal coordination to accomplish desired mission goals. Considering this, Distributed Satellite Systems (DSS) is a promising concept

for the future of SSA and STM. DSS mission architectures move away from the monolith system concept to adopt multiple elements that interact, cooperate, and communicate with each other leading to new systemic properties and/or emerging functions [9], [10]. DSS can be classified into different types, such as constellations[11], clusters, swarms, trains, fractionated spacecraft, and federated satellites [12]–[14]. In contrast to the conventional ground-based systems whose observations are conducted from accurately surveyed locations, SBSS platforms are subjected to positional errors and tracking errors caused by onboard TSPI/Navigation systems and tracking sensors respectively. These errors can be represented geometrically in the form of ellipsoids which can be combined to form the total uncertainty volume that determines the total position uncertainty of the tracked RSO to support Separation Assurance (SA) and Collision Avoidance (CA) [15] which is later on followed by the application of relevant CA maneuvers. In this paper a non-cooperative SBSS scenario is analyzed, in which DSS spacecrafts track a RSO subject to specific errors in tracking and navigation systems for positioning that will ultimately determine the uncertainty volume.

## 2. AIM OF THE ARTICLE

This article addresses tracking and detection of RSO using vision-based sensors with an aim to realize trusted autonomy in heterogenous DSS platforms for autonomous navigation and CA capabilities to achieve SDA. The remaining article is structured as follows. Section 3 describes the SBSS mission concept and system architecture. Section 4 defines the triangulation problem, equations corresponding to the triangulation problem and the Particle Swarm Optimization (PSO) algorithm. Section 5 presents the results and discussion obtained from the verification case studies. Section 6 comprises conclusions and scope for future research.

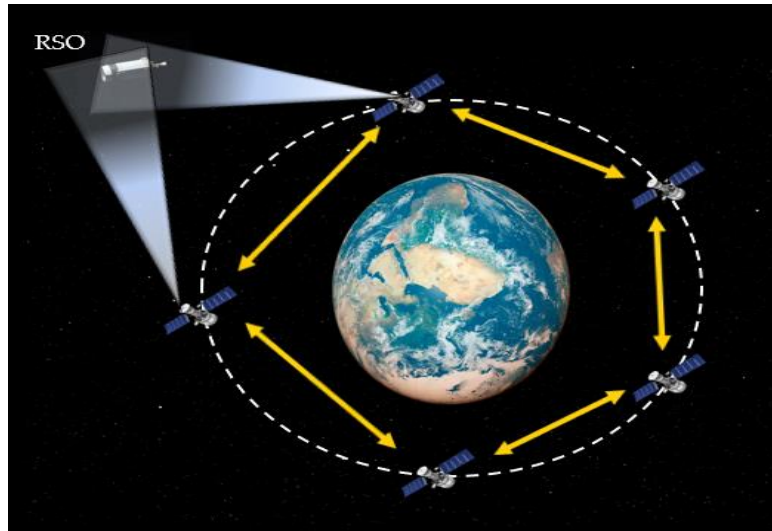


Figure 2. SBSS mission concept employing DSS.

### 3. SBSS MISSION ARCHITECTURE

Recent studies have investigated the use of star trackers as an alternative sensor for monitoring debris[16]. The participating spacecrafts in the DSS are assumed to simultaneously perform Earth observation operations and debris tracking for SBSS. The major focus is to come up with a suitable mission architecture that accomplishes SSA mission objectives expeditiously. The mission architecture is scrutinized based on the following criteria.

- The proposed system configuration must be flexible to support multiple applications envisioned in the future, for instance, point-to-point suborbital transport.
- As opposed to conventional satellite systems, DSS satellites should form an ad-hoc or optional teams that make autonomous decisions and maximize mission objectives without involving the ground control segment.

As illustrated in Figure 2, the participating spacecrafts in the DSS are placed in a nearly circular LEO orbit at an altitude of 400 km, which results in a federated system configuration that tracks and detects RSO autonomously. It is possible to extend the current DSS architecture by placing multiple satellites in more than one orbital plane, thus taking advantage of a wide variety of occurrences and visibility conditions during observations.

For the proposed SBSS mission architecture the following assumptions are adopted: (1) the star trackers on board track the RSO's with the stars in the background; (2) the participating spacecrafts are equipped with GPS for positioning and navigation that provide full set of navigation data; (3) the RSO position is estimated by simultaneous

optical measurements obtained from two different spacecrafts; (4) the participating spacecrafts share their position information and the estimated RSO position through a network; and (5) mutual separation between the spacecrafts belonging to the DSS constellation is guaranteed using intersatellite links and continuous monitoring from the ground stations.

The proposed autonomous navigation system comprises of the following components:

- **Navigation hardware** comprises of the state-of-the-art GPS to obtain a full set of navigation data comprising of the DSS satellites positions, velocities, and attitude rates.
- **Tracking hardware** comprises of star trackers that track the RSO by simultaneous optical measurements.
- The obtained data from the hardware is used as inputs by the **On-Board System (OBS)** to obtain the RSO position estimates, error measurement budget and to generate the uncertainty ellipsoids.
- The **guidance system** exploits the data generated by the OBS for trajectory planning and optimization to generate the steering commands.
- **Actuators** use the steering commands to perform the collision avoidance maneuvers in order to avoid a collision with the RSO.

Figure.3 illustrates the system architecture and its individual components.

### 4. SBSS TRACKING ALGORITHM

A single angles-only sensor is inadequate to obtain range information. In contrast, using two angles-only sensors

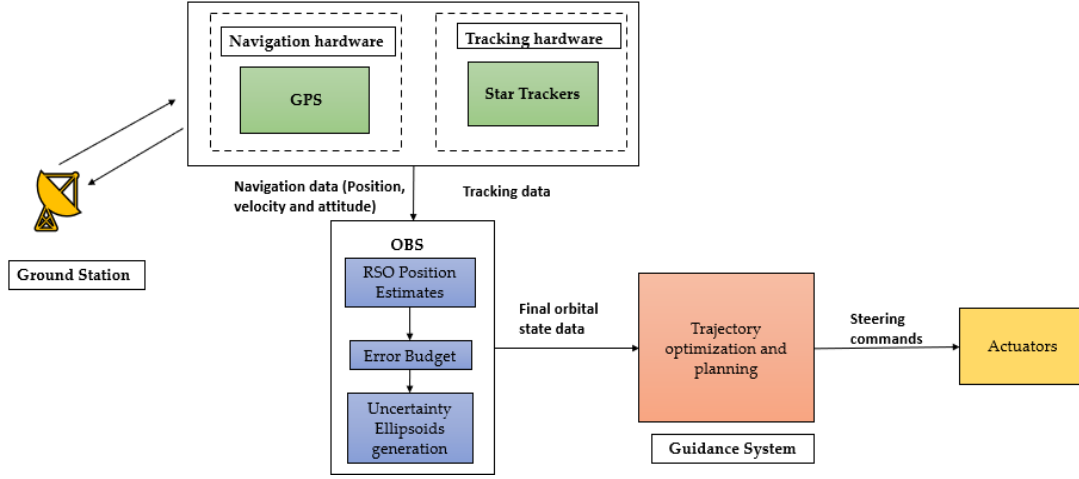


Figure 3. Space debris Collision Avoidance (CA) system architecture.

allows one to determine the range and thus the 3D location of an object via simple triangulation [17], [18]. Since the sensors do not exactly point towards the RSO, an error in the sensor measurement always prevails, so it is necessary to find the most probable RSO position. In the absence of measurement error, triangulation becomes trivial. The current section introduces a suitable tracking algorithm to track the RSO and the corresponding equations required to estimate the position of the RSO, and the errors associated with the measurements. The resulting errors from the triangulation equations are represented in the form of co-variance matrices which are further used to generate the total uncertainty volume.

To determine the 3D location of a RSO, the information regarding the sensor location Line of Sight (LOS) azimuth and elevation pointing angles is necessary. Errors in the knowledge of these ten parameters will lead to an inaccurate 3D position estimate of the RSO. Furthermore, the relationship between measurement error and errors in the estimated target location is a function of the sensor-target-sensor geometry, where a sensor-target-sensor separation of  $90^\circ$  results in the lowest error sensitivity, while a sensor separation of  $0^\circ$  or  $180^\circ$  results in impossible solutions (as seen from the target). To define the triangulation problem, we need to define the positions of the sensors and the RSO in a right-handed coordinate system as illustrated in Figure.4. The

$x$  and  $y$  axis forms the horizontal plane and  $z$  axis pointing out of plane vertically with Earth's centre as the origin.  $\theta_1$  and  $\theta_2$  are the azimuth angles of the corresponding sensors measured clockwise measured from positive  $y$  axis towards positive  $x$  axis. The corresponding elevation angles are denoted by  $\phi_1$  and  $\phi_2$  which increases from  $0^\circ$  in  $xy$  plane to  $90^\circ$  pointing vertically. The horizontal ranges from the  $x$ - $y$  components of the sensor to the  $x$  and  $y$  components of the RSO are denoted by  $r_1$  and  $r_2$  respectively. The separation angle  $\theta_{sep}$  is measured from sensor 1 through RSO to sensor 2. The sensor positions  $(x_1, y_1, z_1)$ ,  $(x_2, y_2, z_2)$  and the Line of Sight (LOS) from sensor to target allows the 3D target position computation. The equations that relate the target location  $(x_t, y_t, z_t)$  to measurements of the sensor position and LOS from the sensors to the target aiding the target position estimation are defined below [18].

$$x_t = \frac{x_2 \tan(\theta_1) - x_1 \tan(\theta_2) + (y_1 - y_2) \tan(\theta_1) \tan(\theta_2)}{\tan(\theta_1) - \tan(\theta_2)} \quad (1)$$

$$y_t = \frac{y_1 \tan(\theta_1) - y_2 \tan(\theta_2) + (x_2 - x_1) \tan(\theta_1) \tan(\theta_2)}{\tan(\theta_1) - \tan(\theta_2)} \quad (2)$$

$$r_1 = \sqrt{(x_i - x_t)^2 + (y_i - y_t)^2} \quad (3)$$

$$z_t = \frac{r_1 \tan(\phi_1) + z_1 + r_2 \tan(\phi_2) + z_2}{2} \quad (4)$$

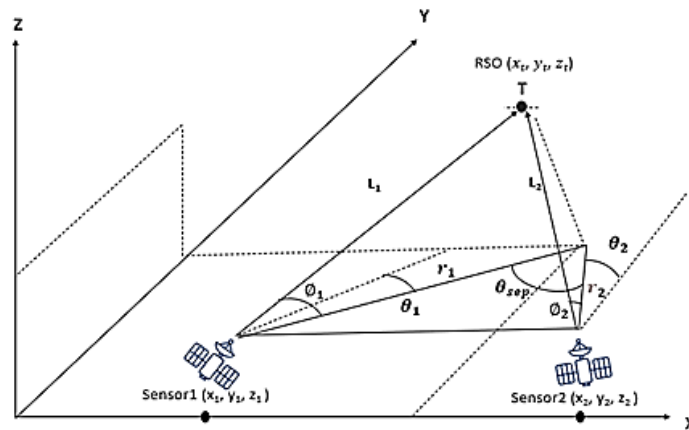


Figure 4. Geometry for Multi-sensor RSO tracking.

The error propagation equations corresponding to the respective position coordinates are derived in [19] with a key assumption that the error generated by each sensor follows gaussian distribution. The sigmas for each  $x_t, y_t, z_t$  are complex sums of various partial derivatives that are further simplified in [20].

$$\sigma_{xt} = \sqrt{c_{x,p}^2 \sigma_p^2 + (rc_{x,\theta})^2 \sigma_\theta^2} \quad (5)$$

$$\sigma_{yt} = \sqrt{c_{y,p}^2 \sigma_p^2 + (rc_{y,\theta})^2 \sigma_\theta^2} \quad (6)$$

$$\sigma_{ri} = \sqrt{c_{r,p}^2 \sigma_p^2 + (rc_{r,\theta})^2 \sigma_\theta^2} \quad (7)$$

$$\sigma_{zt} = \sqrt{c_{z,r}^2 \sigma_r^2 + \sigma_p^2 + (rc_{z,\emptyset})^2 \sigma_\emptyset^2} \quad (8)$$

The various  $c$ 's mentioned in the equations are the error coefficients. For instance, the  $c_{x,p}$  indicates the error coefficient for the x coordinate of the target position.  $c_{x,\theta}$  corresponds to error coefficient for azimuth error in  $x_t$ . Equations (5)-(8) relate the target position uncertainties to the standard deviation in measurement errors  $\sigma_p, \sigma_\theta, \sigma_\emptyset$  where,  $\sigma_p$  is the standard deviation in the position measurement.  $\sigma_\theta$  is the standard deviation in the azimuth measurement.  $\sigma_\emptyset$  is the standard deviation in the elevation measurement. Equation (8) indicates the error in single sensor measurement of  $z_t$ . But since the tracking of the RSO during triangulation is performed using two sensors, the error estimate is calculated as follows:

$$\sigma_{zt} = \frac{1}{2} \sqrt{\sigma_{zt}^2(1) + \sigma_{zt}^2(2) + 2 \frac{\partial z_t}{\partial r_1} \frac{\partial z_t}{\partial r_2} \text{Cov}(\delta r_1, \delta r_2)} \quad (9)$$

$$\text{where: } \text{Cov}(\delta r_1, \delta r_2) = \frac{\partial r_1}{\partial x_t} \frac{\partial r_2}{\partial x_t} \sigma_{x_t}^2 + \frac{\partial r_1}{\partial y_t} \frac{\partial r_2}{\partial y_t} \sigma_{y_t}^2 \quad (10)$$

The steps for obtaining the covariance matrix corresponding to the navigation error are described in detail in the literature[15]. In this case, an on-board GNSS system is assumed to be providing navigational measurements, and the uncertainty values are derived from an experiment on LEO GPS accuracy published in literature [21]. The tracking error can be expressed in terms of the associated co-variance matrix:

$$Q_{TRK} = \begin{bmatrix} \sigma_{x_t}^2 & 0 & 0 \\ 0 & \sigma_{y_t}^2 & 0 \\ 0 & 0 & \sigma_{z_t}^2 \end{bmatrix} \quad (11)$$

Where  $\sigma_x^2, \sigma_y^2, \sigma_z^2$  are obtained using equations (5), (6), (9). The total co-variance matrix is determined by using the Gauss Helmert formulation [22], [23] in order to relate the sensor measurement errors ( $\sigma_{p1}, \sigma_{p2}, \sigma_{\theta1}, \sigma_{\theta2}, \sigma_{\emptyset1}, \sigma_{\emptyset2}$ ) to final RSO position ( $x_t, y_t, z_t$ ). The vectors of estimated observations and estimated parameters are denoted as  $L, X$  respectively and contain the following elements:

$$L = [x_1, y_1, z_1, \theta_1, \varphi_1, x_2, y_2, z_2, \theta_2, \varphi_2]^T \quad (12)$$

$$X = [x_t, y_t, z_t]^T \quad (13)$$

The total co-variance matrix can then be expressed as

$$Q_{TOT(3 \times 3)} = B C_r B^T \quad (14)$$

Where  $C_r$  is the co-variance matrix of the observations. For matrix B the function  $F(X, L) = 0$  needs to be defined.

$$\begin{aligned} x_t - \frac{x_2 \tan(\theta_1) - x_1 \tan(\theta_2) + (y_1 - y_2) \tan(\theta_1) \tan(\theta_2)}{\tan(\theta_1) - \tan(\theta_2)} &= 0; \\ y_t - \frac{y_1 \tan(\theta_1) - y_2 \tan(\theta_2) + (x_2 - x_1) \tan(\theta_1) \tan(\theta_2)}{\tan(\theta_1) - \tan(\theta_2)} &= 0; \\ z_t - \frac{r_1 \tan(\emptyset_1) + z_1 + r_2 \tan(\emptyset_2) + z_2}{2} &= 0 \end{aligned} \quad (15)$$

Then B can be defined as  $\frac{\partial F}{\partial L}$  which gives rise to a  $3 \times 10$  matrix. The feasibility of performing on-board optimization routine depends on computation time and cost. Hence PSO technique is chosen as a primary optimization routine due to its capability of global convergence and robustness to solve highly non-linear problems with greater computational efficiency. Moreover, this technique is used widely to solve diverse spacecraft trajectory optimization problems and its on-board implementation was verified through various case studies for adequate convergence time and low computation cost [24], [25]. The particles move iteratively until they converge onto a global optimal solution considering the goal of optimality, minimizing the cost function which describes the quality of the solution and the imposed constraints. The position of the particles iterates according to:

$$X_i^{(k+1)} = X_i^{(k)} + V_i^{(k+1)} \quad (16)$$

where  $V_i^{k+1}$  is the velocity required to move from  $k^{\text{th}}$  iteration to  $(k+1)^{\text{th}}$  iteration, which is given by:

$$V_i^{k+1} = V_i^k + c_1 \cdot r_1 \cdot (p_i^k - x_i^k) + c_2 \cdot r_2 \cdot (p_g^k - x_i^k) \quad (17)$$

where:

$p_i^k$  is the best position of particle i at time k;

$p_g^k$  is the global best solution for all particles at time k;

$r_1$  and  $r_2$  are random numbers between 0 and 1;

$c_1$  and  $c_2$  are cognitive and scaling parameters respectively and are assigned with a value 2.

Typically, satellite motion in an orbit can be modelled using the classical orbital elements based on Gaussian variational equations. However, these equations result in ambiguity in certain scenarios especially, for the orbits with low eccentricities or inclinations [26]. In order to avoid this ambiguity a new model is used that employs a set of Modified Equinoctial Parameters (MEE) [27] that include second order zonal harmonics or  $J_2$  perturbation effects (i.e. change in Right Ascension of the Ascending Node (RAAN) and argument of perigee with time), specifically the set of MEE developed in [28] are adopted to solve the low thrust transfer problem. The optimal CA maneuver is chosen based on models that are incorporated into the PSO algorithm[29].



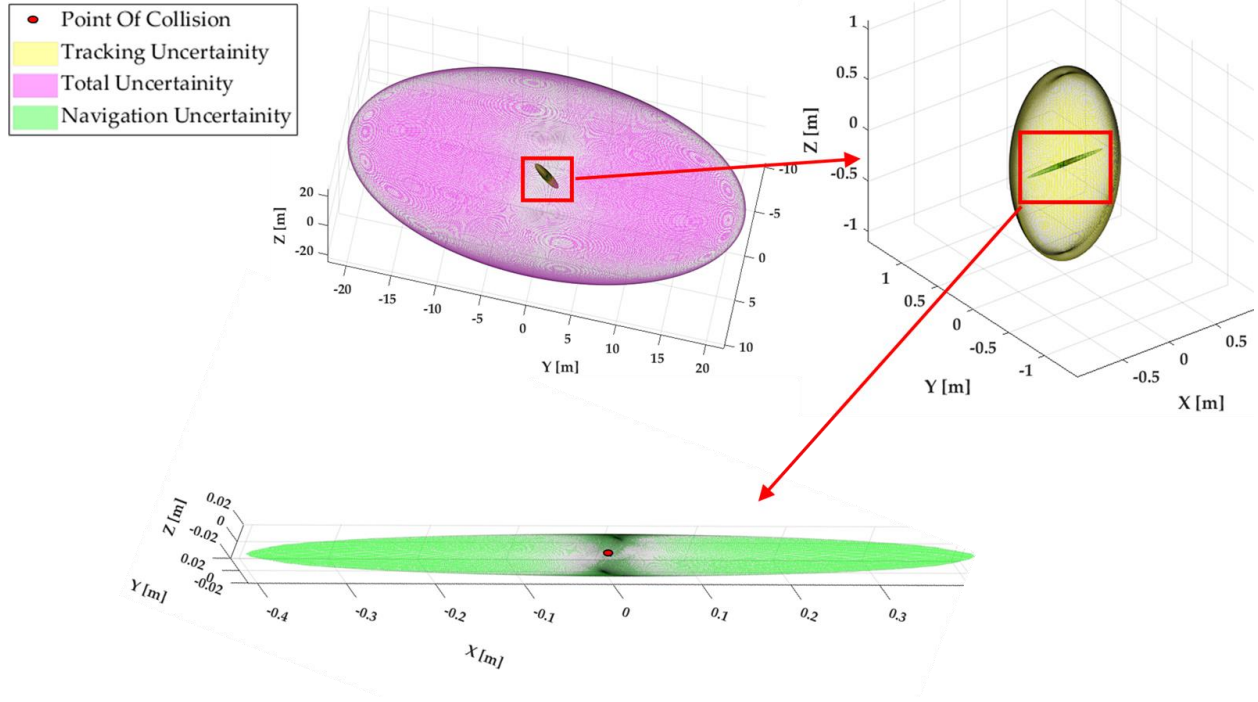


Figure 5. Uncertainty Volumes in SBSS.

## 5. RESULTS AND DISCUSSIONS

The results obtained from the simulation case study in the SBSS scenarios are discussed in this section. To estimate the target position using the algorithm defined in section 4, we define the satellite orbital elements in ECI frame (Table 1) and a conversion to cartesian frame is performed (Table 2).

Table 1. Sensor orbital state elements.

Orbital parameters	Sensor 1	Sensor 2
$a$ (km)	6778	6778
$e$	0.002	0.002
$i$ (deg)	100	100
$\omega$ (deg)	20	20
$\Omega$ (deg)	360	360
$\theta$ (deg)	0	72

Table 2. Corresponding sensor state vectors

Cartesian Coordinates	Sensor 1	Sensor 2
$X_i$ (km)	6356.49	-236.40
$Y_i$ (km)	-401.74	-1175.53
$Z_i$ (km)	2278.42	6666.81
$VX$ (km/sec)	-2.62	-7.69
$VY$ (km/sec)	-1.25	0.043
$VZ$ (km/sec)	7.11	-0.249
Azimuth (deg)	20	300
Elevation (deg)	50	45

The target position estimates, and the ranges obtained from the algorithm are tabulated in Table 3.

Table 3. RSO position estimates in km.

$x_t$	$y_t$	$z_t$	$R_1$	$R_2$	$L_1$	$L_2$
4978.9	-4186.6	9883.7	4027	6022.1	8606.01	6827.4

The values of the corresponding error coefficients must be computed to calculate the errors in the target position estimates. The error coefficients are complex sums of partial derivatives that are simplified in [19]. The sigmas for each  $x_t$ ,  $y_t$ ,  $z_t$  are calculated using Equations (5) to (10).

Table 4. Error estimates for target position parameters.

Sigmas	$x_t$ (km)	$y_t$ (km)	$r$ (km)	$z_t$ (km)
Total Error (m)	10	22	18	24

Assuming that the state-of-the-art star trackers can provide the sigma position  $\sigma_p = 0.5m$ , sensor angular error  $\sigma_\theta = 0.0022$  degrees we obtain the sigmas tabulated in Table 4. Figure 5 illustrates the uncertainty ellipsoid corresponding to navigation, tracking, and total errors. The DSS performs a collision avoidance maneuver to reorient its initial orbit to a modified orbit with a semimajor axis increased to 10 km to avoid the uncertainty volume. It is assumed that the spacecraft that performs the orbit raising maneuver is equipped with Nano Avionics: EPSSC1 that can generate a thrust of 1N with a specific impulse of 213 seconds [30]. Table 5 tabulates the orbital parameters of the spacecraft before and after the maneuver.

**Table 5. Initial and final orbital parameters of the spacecraft after collision avoidance maneuvers.**

Orbital parameter	Initial state	Final state
a(km)	6778	6788
e	0.002	0.002
i(deg)	100	100
$\omega$ (deg)	20	20
$\Omega$ (deg)	360	360

The solution converged after 1,884,000 iterations with a total run time of 16,763 seconds in a MATLAB environment on an Intel Core i7 7<sup>th</sup> generation processor.

**Table 6. Generated control parameters for thrust directions.**

$t_f$ (min)	$\alpha_M$ (deg)	$\beta_M$ (deg)	$f_T$	$k_T$ (rad)	$p_1$	$p_2$
55.19	-2.5	3.08	0.5	0.194	0.19	1

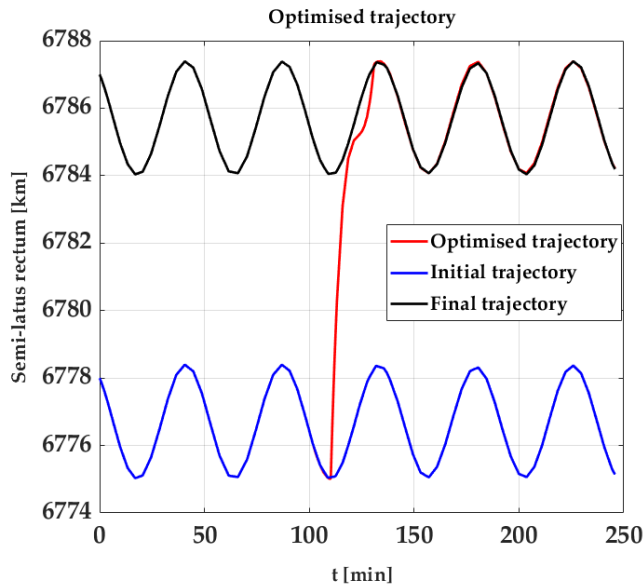


**Figure 6. Change in Semi major axis from initial to final trajectory in time (SBSS).**

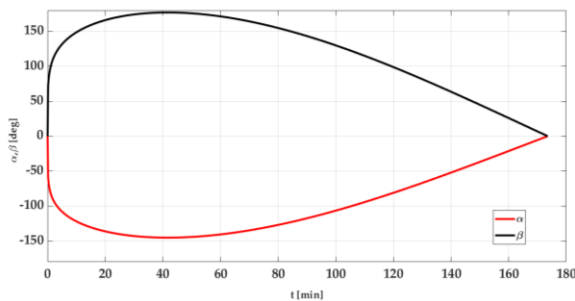


**Figure 7. Change in Thrust control angles in time.**

The change from the initial trajectory to the final optimal

trajectory is illustrated in Figure 6 and the control parameters for the constant thrust directions illustrated in Figure 7 are tabulated in Table 6 for the SBSS scenario.

## 6. CONCLUSION AND FUTURE WORK

The research presented in this article addressed the envisioned implementation of Distributed Satellite Systems (DSS) in a Space-Based Space Surveillance (SBSS) mission using star trackers in the context of Space Domain Awareness (SDA) for Space Traffic Management (STM). In order to obtain range data, the measurements from single angle-only sensors are insufficient. In contrast, performing triangulation using simultaneous measurements from multiple sensors provides a satisfactory solution for the tracking problem. Following this, the satellite can perform a CA maneuver with the help of the host platform. A simulation case study is presented in the SBSS scenario, and the results substantiate the validity of the proposed mathematical framework. Current research is addressing the development of Artificial Intelligence (AI)-based autonomous navigation/guidance algorithms and integration of SBSS and ground-based tracking sensors towards maximizing DSS performance in different applications and operational conditions.

## REFERENCES

- [1] M. J. Holzinger and M. K. Jah, "Challenges and Potential in Space Domain Awareness," *J. Guid. Control Dyn.*, vol. 41, pp. 15–18, Jan. 2018, doi: 10.2514/1.G003483.
- [2] "Space Environment Statistics · Space Debris User Portal." <https://sdup.esoc.esa.int/discosweb/statistics/> (accessed Jul. 16, 2022).
- [3] S. Hilton, R. Sabatini, A. Gardi, H. Ogawa, and P. Teofilatto, "Space traffic management: towards safe and unsegregated space transport operations," *Prog. Aerosp. Sci.*, vol. 105, pp. 98–125, Feb. 2019, doi: 10.1016/j.paerosci.2018.10.006.
- [4] M. R. Ackermann, R. Kiziah, P. C. Zimmer, J. McGraw, and D. Cox, "A systematic examination of ground-based and space-based approaches to optical detection and tracking of satellites," in *31st Space Symposium*, 2015.
- [5] T. Flohrer, H. Krag, H. Klinkrad, and T. Schildknecht, "Feasibility of performing space surveillance tasks with a proposed space-based optical architecture," *Adv. Space Res.*, vol. 47, no. 6, pp. 1029–1042, Mar. 2011, doi: 10.1016/j.asr.2010.11.021.
- [6] X. Vanwijck and T. Flohrer, "Possible contribution of space-based assets for space situational awareness," *Int. Astronaut. Fed. - 59th Int. Astronaut. Congr. 2008 IAC 2008*, vol. 4, pp. 2466–2472, Jan. 2008.
- [7] H. Yunpeng, L. Kebo, L. Yan'gang, and C. Lei, "Review on strategies of space-based optical space situational awareness," *J. Syst. Eng. Electron.*, vol. 32, no. 5, pp. 1152–1166, Oct. 2021, doi: 10.23919/JSEE.2021.000099.
- [8] R. Sabatini, M. Battipede, and F. Cairola, "Innovative Techniques for Spacecraft Separation Assurance and Debris Collision Avoidance," 2020.

- [9] C. Araguz, E. Bou-Balust, and E. Alarcón, "Applying autonomy to distributed satellite systems: Trends, challenges, and future prospects," *Syst. Eng.*, vol. 21, Mar. 2018, doi: 10.1002/sys.21428.
- [10] J. Le Moigne, J. C. Adams, and S. Nag, "A New Taxonomy for Distributed Spacecraft Missions," *IEEE J. Sel. Top. Appl. Earth Obs. Remote Sens.*, vol. 13, pp. 872–883, 2020, doi: 10.1109/JSTARS.2020.2964248.
- [11] K. Hussain, K. Hussain, S. Carletta, and P. Teofilatto, *Deployment of a microsatellite constellation around the Moon using chaotic multi body dynamics*. 71st International Astronautical Congress (IAC), Dubai, United Arab Emirates, 25-29 October 2021.
- [12] M. K. Ben-Larbi *et al.*, "Towards the automated operations of large distributed satellite systems. Part 1: Review and paradigm shifts," *Adv. Space Res.*, vol. 67, no. 11, pp. 3598–3619, Jun. 2021, doi: 10.1016/j.asr.2020.08.009.
- [13] O. von Maurich and A. Golkar, "Data authentication, integrity and confidentiality mechanisms for federated satellite systems," *Acta Astronaut.*, vol. 149, pp. 61–76, Aug. 2018, doi: 10.1016/j.actaastro.2018.05.003.
- [14] A. Golkar, "Federated satellite systems (FSS): a vision towards an innovation in space systems design," in *IAA Symposium on Small Satellites for Earth Observation*, 2013.
- [15] S. Hilton, F. Cairola, A. Gardi, R. Sabatini, N. Pongsakornsathien, and N. Ezer, "Uncertainty quantification for space situational awareness and traffic management," *Sensors*, vol. 19, no. 20, p. 4361, 2019.
- [16] I. Ettouati, D. Mortari, and T. Pollock, "Space surveillance using star trackers. Part I: Simulations," *Pap. AAS*, pp. 06–231, 2006.
- [17] L. Chen, C. Liu, Z. Li, and Z. Kang, "A New Triangulation Algorithm for Positioning Space Debris," *Remote Sens.*, vol. 13, no. 23, p. 4878, Dec. 2021, doi: 10.3390/rs13234878.
- [18] J. N. Sanders-Reed, "Impact of tracking system knowledge on multisensor 3D triangulation," presented at the AeroSense 2002, Orlando, FL, Jul. 2002, pp. 33–41. doi: 10.1117/12.472599.
- [19] J. N. Sanders-Reed, "Error propagation in two-sensor three-dimensional position estimation," *Opt. Eng.*, vol. 40, no. 4, pp. 627–636, 2001.
- [20] J. N. Sanders-Reed, "Triangulation Position Error Analysis for Closely Spaced Imagers," presented at the SAE 2002 World Congress & Exhibition, Mar. 2002, pp. 2002-01-0685. doi: 10.4271/2002-01-0685.
- [21] I. GNSS, "GPS Receiver Performance On Board a LEO Satellite," *Inside GNSS - Global Navigation Satellite Systems Engineering, Policy, and Design*, Jul. 21, 2014. <https://insidegnss.com/gps-receiver-performance-on-board-a-leo-satellite/> (accessed Oct. 07, 2022).
- [22] G. R. Curry, "radar System Performance Modeling, ARTECH HOUSE," *Inc Ed Norwood MA USA*, 2005.
- [23] D. A. Vallado, *Fundamentals of astrodynamics and applications*, vol. 12. Springer Science & Business Media, 2001.
- [24] M. Lin, Z.-H. Zhang, H. Zhou, and Y. Shui, "Multiconstrained Ascent Trajectory Optimization Using an Improved Particle Swarm Optimization Method," *Int. J. Aerosp. Eng.*, vol. 2021, 2021.
- [25] A. Rahimi, K. Dev Kumar, and H. Alighanbari, "Particle Swarm Optimization Applied to Spacecraft Reentry Trajectory," *J. Guid. Control Dyn.*, vol. 36, no. 1, pp. 307–310, 2013, doi: 10.2514/1.56387.
- [26] J. T. Betts, *Practical Methods for Optimal Control and Estimation Using Nonlinear Programming, Second Edition*. Society for Industrial and Applied Mathematics, 2010. doi: 10.1137/1.9780898718577.
- [27] G. Baù, J. Hernando-Ayuso, and C. Bombardelli, "A generalization of the equinoctial orbital elements," *Celest. Mech. Dyn. Astron.*, vol. 133, no. 11, pp. 1–29, 2021.
- [28] S. Eves, "Applied Nonsingular Astrodynamics: Optimal Low-Thrust Orbit Transfer J. A. Kéchichian Cambridge University Press, University Printing House, Shaftesbury Road, Cambridge CB2 8BS, UK. 2018. xvii; 461 pp. ISBN 978-1-108-47236-4," *Aeronaut. J.*, vol. 124, no. 1282, pp. 2036–2037, Dec. 2020, doi: 10.1017/aer.2020.105.
- [29] E. Lagona, S. Hilton, A. Afful, A. Gardi, and R. Sabatini, "Autonomous Trajectory Optimisation for Intelligent Satellite Systems and Space Traffic Management," *Acta Astronaut.*, vol. 194, pp. 185–201, May 2022, doi: 10.1016/j.actaastro.2022.01.027.
- [30] "CubeSat Propulsion System EPSS," *NanoAvionics*. <https://nanoavionics.com/cubesat-components/cubesat-propulsion-system-epss/> (accessed Jan. 02, 2023).

## BIOGRAPHY



**Khaja Faisal Hussain** has received his joint bachelor's degree from GRIET, India and Karabuk University, Turkey. He graduated with his master's in aerospace engineering from Sapienza University of Rome, Italy and is currently pursuing a PhD in Aerospace engineering at Khalifa University, UAE. His current research deals with Autonomous Systems for Space Domain Awareness (SDA) and Distributed Satellite Systems (DSS).



**Kathiravan Thangavel** is a Ph.D candidate at RMIT University's Cyber-Physical and Autonomous System Research Group, and his research is funded by SmartSat CRC and the Andy Thomas Space Foundation. He graduated from Anna University in Chennai, India, with a bachelor's degree in aeronautical engineering. Following that, he pursued a master's degree in Aerospace Engineering at Rome's La Sapienza University. Kathiravan completed the International Space University Space Studies Program 2019. He is excited about research in space and the potential of exploring space to the benefit of humanity, and



*his key areas of interest are Distributed Satellite Systems, Artificial Intelligence, Autonomy, Earth Observation, Space Domain Awareness, Space Traffic Management, Thermomechanical Analysis.*



**Dr. Alex Gardi** obtained his BSc and MSc degrees in Aerospace Engineering from Politecnico di Milano (Italy) and a PhD in the same discipline from RMIT University (Australia). Dr Gardi is currently an Assistant Professor at Khalifa University (UAE) and Associate of RMIT University, focusing on aerospace cyber-physical systems (UAS, satellites, ATM systems and avionics). In this domain, he specialises in multi-objective trajectory optimization with emphasis on optimal control methods, multidisciplinary design optimization and AI/metaheuristics for air and space platforms.



**Dr. Rob Sabatini** is a Professor of Aeronautics and Astronautics with three decades of experience in Aerospace, Defense and Robotics/ Autonomous Systems research and education. Prof. Sabatini holds a PhD in Aerospace/Avionics Systems (Cranfield University) and a PhD in Space Geodesy/Satellite Navigation (University of Nottingham). His research addresses key contemporary issues in digital and sustainable aerospace systems design, testing and certification, with a focus on: Avionics and CNS/ATM; Autonomous Navigation and Guidance; Unmanned Aircraft Systems; Distributed Space Systems; Space Domain Awareness and Space Traffic Management.